Molecular Modeling of the Aldose Reductase-Inhibitor Complex Based on the X-ray Crystal Structure and Studies with Single-Site-Directed Mutants

Suresh B. Singh,*,† Michael S. Malamas,† Thomas C. Hohman,† Ramaswamy Nilakantan,†
Deborah A. Carper,‡ and Douglas Kitchen†,§

Wyeth Ayerst Research, CN 8000, Princeton, New Jersey 08543-8000, and National Eye Institute, NIH, 9000 Rockville Pike, Bethesda, Maryland 20892

Aldose reductase (AR) has been implicated in the etiology of the secondary complications of diabetes. This enzyme catalyzes the reduction of glucose to sorbitol using nicotinamide adenine dinucleotide phosphate as an essential cofactor. AR has been localized at the sites of tissue damage, and inhibitors of this enzyme prevent the development of neuropathy, nephropathy, retinopathy, and cataract formation in animal models of diabetes. The crystal structure of AR complexed with zopolrestat, a potent inhibitor of AR, has been described.[1] We have generated a model of the AR-inhibitor complex based on the reported Cα coordinates of the protein and results of a structure–activity relationship study using four structurally distinct classes of inhibitors, recombinant human AR, and four single-site-directed mutants of this enzyme. The effects of the site-directed mutations on residues within the active site of the enzyme were evaluated by average interaction energy calculations and by calculations of carbon atom surface area changes. These values correlated well with the IC_{50} values for zopolrestat with the wild-type and mutant enzymes, validating the model. On the basis of the zopolrestat-binding model, we have proposed binding models for 10 other AR inhibitors. Our models have enabled us to gain a qualitative understanding of the binding domains of the enzyme and how different inhibitors impact the size and shape of the binding site.

Introduction

The polyol pathway has been implicated in the etiology of the secondary complications of diabetes. Inhibitors of aldose reductase, the first enzyme in the pathway, block the flux of glucose through the pathway and, in animal models of diabetes, prevent or reverse functional deficits and structural damage in the lens, retina, kidney, and peripheral nerves. However, in human studies, with few exceptions, these compounds have produced little evidence of clinical benefit and some have produced adverse effects, prompting efforts to design more potent and specific inhibitors.

X-ray crystallographic studies have shown that aldose reductase inhibitors occupy the active site of the human enzyme[1–3] where inhibitor binding is a consequence of polar and nonpolar interactions between the inhibitor and the complementary residues that line the enzyme binding pocket. To test the potential role of active-site residues in inhibitor binding and activity, we have prepared mutations of two active-site apolar residues thought to play dominant roles in the binding of the inhibitor zopolrestat, tryptophan 20 and 111, and have tested these mutants with representative compounds from four structurally distinct series of aldose reductase inhibitors (Table 1). To help distinguish the effects resulting from changes in residue size

from those secondary to changes in lipophilicity, tryptophan 20 and 111 were replaced with both alanine and tyrosine.

To understand the results of the mutation studies we attempted to develop active-site models of each of the inhibitors bound to the native and mutant proteins. Cocrystallization of the inhibitors or extensive computer simulations were impractical for all the 55 possible complexes. Therefore, we used rapid docking techniques for the analysis of these complexes. Based on the Cα coordinates of the AR:zopolrestat complex published by Wilson et al.[1] we have created a model of the enzyme–inhibitor complex. Using this model along with an automated docking procedure entitled SHAPE SEARCH,[4] we have generated binding models for other AR inhibitors. We have also used the AR:zopolrestat complex to model the W20 and W111 mutants.[5] We evaluated the inhibitor binding models using carbon atom surface area (CSA) change calculations to estimate the change in the free energy of transfer of inhibitors from solvent into the mutant protein active site relative to that of the native protein. To compare the results of CSA calculations we evaluated average interaction energies as a measure of relative binding affinities of zopolrestat with the native and mutant enzymes with molecular dynamics/free energy perturbation calculations.

Methods

The starting structure for the aldose reductase: NADP+:zopolrestat quaternary complex contained the Cα coordinates for aldose reductase, the cofactor NADP+,

---

* Corresponding author. Current address: Merck Research Laboratories, RY50SW100, P.O. Box 2000, Rahway, NJ 07065. Tel: (732) 594-4954. Fax: (732) 594-4224. E-mail: suresh_singh@merck.com.
† Wyeth Ayerst Research.
‡ National Eye Institute.
§ Current address: Albany Molecular Research, Inc., 21 Corporate Circle, Albany, NY 12203.

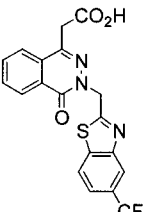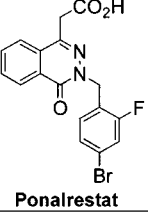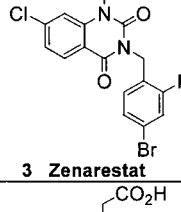**Table 1.** Inhibition of Human Recombinant and Mutant Aldose Reductase by Structurally Distinct Inhibitors
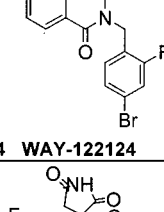
Compound	IC_{50}^{WT} (x10^{-8} M)	IC_{50} ratios ($IC_{50}^{MUT}/IC_{50}^{WT}$)			
		W20Y	W20A	W111Y	W111A
1 Zopolrestat	3.64±0.07	1.3	838	1	387
2 Ponalrestat	6.65±0.04	47	1770	58	1770
3 Zenarestat	4.24±0.04	2.5	448	12	786
4 WAY-122124	22.66±0.73	21	311	193	120
ARI-509	7.26±0.07	0.1	4.6	2.5	413
6 WAY-124276	14.41±0.13	0.1	1	2	19
7 Tolrestat	4.70±0.05	0.25	2244	0.6	4
8 Imirestat	5.47±0.04	48	9141	1960	781

Table 1 (Continued)
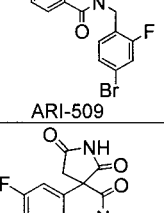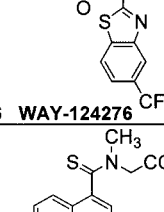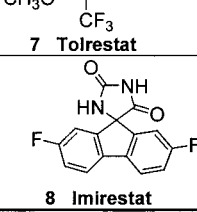
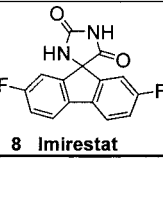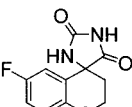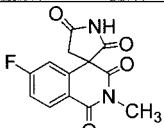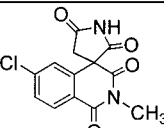| Compound	IC_{50}^{WT} ($\times 10^{-8}$ M)	IC_{50} ratios ($IC_{50}^{MUT}/IC_{50}^{WT}$)			
		W20Y	W20A	W111Y	W111A
9 Sorbinil	91.86±2.43	84	>1089	>1089	>1089
10 WAY-121365	7.32±0.06	3	1673	773	2732
11 WAY-120823	7.82±0.12	1.5	1068	324	>1279

and the inhibitor zopolrestat from Wilson et al.'s crystal structure (PDB accession code: 1mar)[1] and the side chain conformations from the crystal structure of aldose reductase complexed with glucose-6-phosphate and NADPH (PDB accession code: 2acq).[3] We generated the starting structure by merging the coordinates from 1mar and 2acq. These two structures of protein are very similar in conformation except for the structure of residues phe[122]-pro[132], ala[220]-asp[224], and cys[298]-cys[303]. To refine the resulting structure we adopted the following energy minimization protocol: except for the final step, the Cα coordinates of all the residues, zopolrestat, and NADP$^+$ were held in their positions in the crystal structure. (1) In the first step the hydrogen atoms alone were minimized followed by the refinement of the side chains of the three stretches of amino acids identified above. (2) In the second step the backbone was refined. (3) In the third step the backbone and the side chains were minimized. (4) In the fourth step the whole protein was minimized. (5) In the final refinement step the whole complex was allowed to move. All the refinement steps were carried out with 500 steps of minimization (50 steps of steepest descent + 450 steps of conjugate gradient), a distance-dependent dielectric function, and AMBER 3.0 force field.[6] The refined structure was then used to generate the following four mutants: W20A, W20Y, W111A, and W111Y. These structures were subsequently minimized with the conjugate gradient technique in AMBER 4.0.[7] All these structures then served as the starting point for docking inhibitors into the active site.

In all AMBER calculations we used MOPAC AM1 charges for zopolrestat and NADP$^+$. The missing force field parameters for zopolrestat and NADP$^+$ were approximated from AMBER 3.0 force field. The charges and the assigned force field parameters for zopolrestat and NADP$^+$ are given in the Supporting Information.

Automated Docking Calculations Using SHAPE SEARCH.[4] All automated docking calculations were carried out with SHAPE SEARCH. SHAPE SEARCH was derived from a collaborative effort between the Structural Biology group of Lederle Laboratories and the laboratory of Irwin Kuntz at UCSF. The atomic positions of zopolrestat (19 atoms) served as the site points for docking all the inhibitors. Random rotations of single, nonring bonds were used to generate and store different conformations of the ligands. Using a single conformation of zopolrestat as the site points, however, is likely to have eliminated from consideration many of these conformations during the docking procedure.

Matching Procedure. The docking graph method of Crippen and co-workers[8,9] was used to carry out the matching between site points and ligand atoms. In this method, a docking graph is constructed with a node representing every possible docking of the ligand atoms on the site points. For every ligand interatomic distance that matches a site distance, there is an edge in the docking graph connecting the appropriate nodes. Cliques, completely connected subgraphs in the docking graph, are assumed to represent valid dockings of the ligand on the lattice. In this work, fairly stringent tolerances for distance matches (0.25 to 0.5 Å) were used, and the maximum number of orientations was set to 10 000. The docking graph method generates a very large number of possible orientations since only four atoms at a time are considered. Therefore, this technique partly eliminates the bias of using zopolrestat as the shape template.

Each of the possible docked orientations was subjected to rigid body minimization with 50 steps of steepest descent followed by 50 steps of conjugate gradient minimization. If the initial van der Waals energy was too high, then the next orientation was used. The van der Waals 6-12 term was derived by a simple approximation of the van der Waals radii of each element. Charges were estimated using the Gasteiger method[10] for the small molecule inhibitors and were obtained from the AMBER 3.0 force field[6] for the protein. A distance-dependent dielectric was used (R_{ij}) for the electrostatic term. All the hydrogen atoms were included to properly account for hydrogen bonding and other electrostatic effects. The resulting possible orientations were then
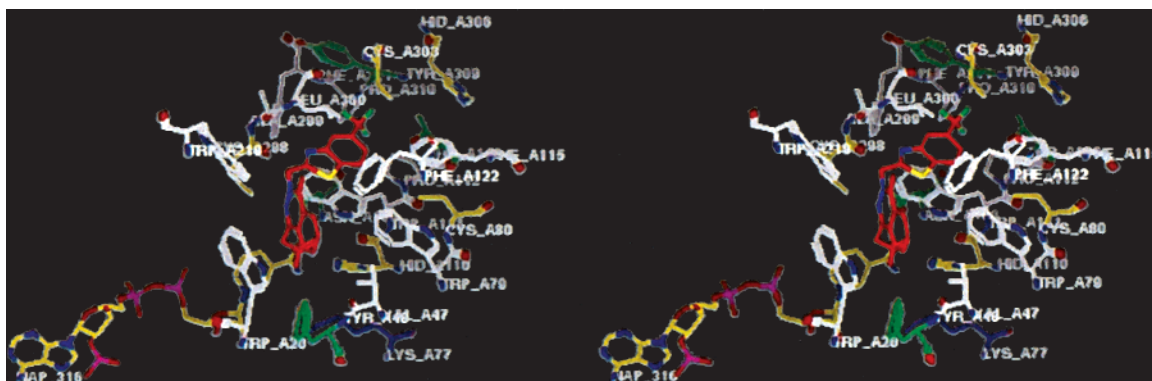
Figure 1. The modeled structure of aldose reductase in complex with zopolrestat and NADP$^+$ shown in stereo.

scored with the following Lennard-Jones and electrostatic scoring function:

$$\sum_{i<j}\left\{\left(\frac{A_{ij}}{R_{ij}^{12}} - \frac{B_{ij}}{R_{ij}^{6}}\right) + \frac{q_i q_j}{\epsilon R_{ij}}\right\}$$

We believe that this simple and efficient scoring scheme is reliable to estimate the structure of bound orientations of small molecules. We did not find the scores useful to predict binding affinities, however. Other measures were found to relate better to the measured IC$_{50}$ values.

Carbon Surface Area Calculations. As an approximate method of estimating lipophilic effects, the accessible surface area of the carbon atoms of the small molecule inhibitors were calculated for each mutant and for each inhibitor. Accessible surface areas were calculated with the IMPACT program[11] using the Connolly surface algorithm.[12]

Average Interaction Energy Calculations. The refined model of the AR:zopolrestat complex was used as a starting point and solvated with a spherical cap of TIP3P·H$_2$O molecules[13] up to 20 Å from tyrosine 48 at the entrance of the active site. This resulted in a spherical cap of 226 waters surrounding the active site. The solvated complex was minimized and then equilibrated for 10 ps at 300 °K as presented elsewhere.[14] The evaluation of average interaction energy between the inhibitor and the wild type relative to that of the mutant was carried out with the equilibrated structure using molecular dynamics/free energy perturbation calculations in forward and backward directions for 10 ps in each direction. In these free energy perturbation calculations we used the thermodynamic windows method with fixed widths.[15] All these calculations were carried out using AMBER 4.0.[7] Each free energy perturbation was carried out by mutating W20 → Y20, W20 → A20, W111 → Y111, and W111 → A111 in the enzyme:NADP$^+$:inhibitor quaternary complex and also in the enzyme:NADP$^+$ binary complex in both the forward ($\lambda = 1 \rightarrow 0$) and backward ($\lambda = 0 \rightarrow 1$) directions. The force field parameters describing tryptophan were changed smoothly and uniformly to tyrosine and alanine in separate free energy perturbation calculations, employing methods described elsewhere.[15]

Since our aim in this study was to confirm the relative rankings of binding affinities from carbon surface area calculations and correlate with them experimentally measured relative IC$_{50}$ values, we used FEP simulations

of short durations to estimate the average interaction energy between the inhibitor and the native enzyme relative to that of the mutant.

Results

The crystal structure of the aldose reductase:zopolrestat:NADP$^+$ complex contains only the Cα coordinates of the protein. We modeled the side chain conformations from the crystal structure of aldose reductase in complex with NADPH and glucose-6-phosphate. The side chain conformations in the aldose reductase:zopolrestat complex (1mar) are very similar to those in the aldose reductase:glucose-6-phosphate complex (2acq) for the majority of the protein (0.28 Å RMSD) except for the residues phe^{122}-pro^{132}, ala^{220}-asp^{224}, and cys^{298}-cys^{303}. The RMS deviation of these three stretches in Cα coordinates in 1mar relative to those in 2acq are 0.41, 0.23, and 0.97 Å, respectively. It is clear from this that the third stretch, cys^{298}-cys^{303}, changes the most in its position relative to the glucose-6-phosphate bound form. Our refinement procedure led to backbone and side chain conformations of these stretches that are consistent with the Cα positions in the zopolrestat complex and similar in side chain conformations (see Figure 1) to those published by Wilson et al.[1] We modeled the conformation of leucine 300 graphically in order to visually match its conformation in the figures published by Wilson et al.[1] In our final refined model, the distance between the Y48 hydroxyl oxygen and the closest carboxylate oxygen of zopolrestat is 2.7 Å, and the distance between the H110 Nϵ to the nearest carboxylate oxygen is 2.8 Å, similar to those observed by Wilson et al.[1] The angle for H110 Nϵ -Hϵ2-carboxylate oxygen of zopolrestat is 135.7°, which is close to that observed in the crystal structure of aldose reducatase:tolrestat complex (139.7°). Thus we are confident that we have regenerated a conformation of aldose reductase in complex with zopolrestat consistent with that of the crystal structure.[1]

We used this structure of the aldose reductase:zopolrestat complex to generate models of the W20Y, W20A, W111Y, and W111A mutants. All the resultant models are essentially similar in structure since we have imposed Cartesian restraints on the movement of zopolrestat in the active site. Models of the inhibitor-bound form of aldose reductase and its mutants were used to carry out automated and manual inhibitor docking studies.

The active-site residues of interest and the predicted mutant structures are shown with the corresponding
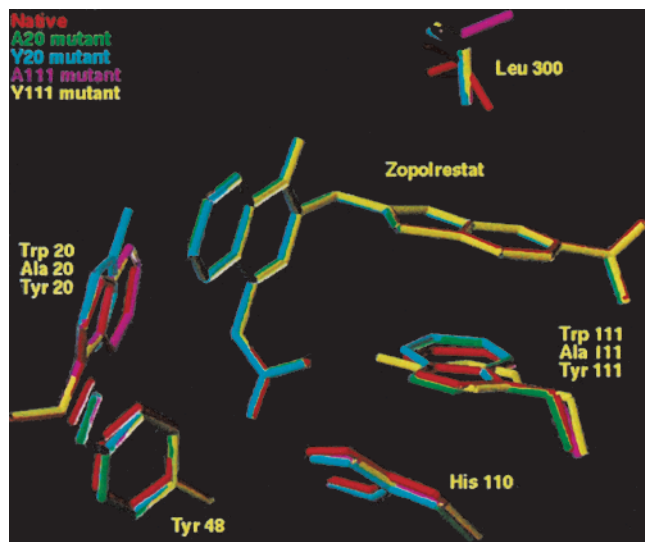
Figure 2. Docked orientations of zopolrestat generated by SHAPE SEARCH in the native and W20A, W20Y, W111A, and W111Y mutants of aldose reductase.

predicted docking orientations of zopolrestat in Figure 2. This view shows that zopolrestat binds in the same orientation in all of the mutant enzymes.

The IC$_{50}$ values of zopolrestat for the native enzyme are shown in Table 1.[5] The table also lists the IC$_{50}$ ratios (IC$_{50}^{MUT}$/IC$_{50}^{WT}$) for each of the inhibitors we have modeled in our study. The inhibitor activity of zopolrestat with the tyrosine 20 mutant is similar to that for zopolrestat with the native enzyme, while that with the alanine 20 mutant is considerably decreased. These observations can be best rationalized with our model if we assume that this mutation affects not only inhibitor affinity but also substrate binding and hence leads to a greater decrease in the apparent IC$_{50}$ than would be expected solely based on tryptophan → alanine mutation. Zopolrestat activity with the tyrosine 111 mutant is also equivalent to that with the native enzyme. Alanine substitution for tryptophan 111, however, decreases the enzyme's affinity for zopolrestat. In our model this residue substitution causes one whole face of zopolrestat's benzothiazole ring to lose its interaction with the indole ring of tryptophan, which likely accounts for the loss of its affinity. A similar trend for changes in inhibitor activity with the enzyme mutants occurs for the first three inhibitors in Table 1: zopolrestat, ponalrestat, and zenarestat. However, for WAY-122124 the effect of W111Y and W111A mutations is comparable, indicating that the size of the tryptophan ring alone is not responsible for its binding.

The spirosuccinimide moiety of ARI-509 and WAY-124276 was designed to mimic the carboxyl acid moiety[16] of the inhibitors described above. The recent crystal structure of sorbinil complexed with porcine aldose reductase presented by Urzhumtsev et al.[2] shows that the spirohydantoin of sorbinil binds in the same oxyanion well as the carboxylate moiety of zopolrestat.[1] Consistent with these observations, our docked models place the spirosuccinimide moiety (a close analogue of the spirohydantoin ring of sorbinil) in the oxyanion hole with the 6-fluoro-4-hydro-isoquinoline-1,3-dione ring opposite W20 (Figure 3). In this orientation, the 2-fluoro-
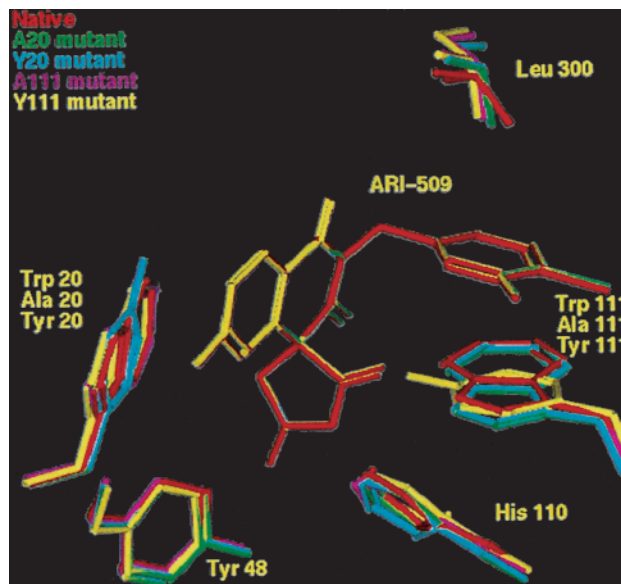

Figure 3. Docked orientations of ARI-509 generated by SHAPE SEARCH in the native and W20A, W20Y, W111A, and W111Y mutants of aldose reductase.

4-bromobenzyl group of ARI-509 is positioned opposite to W111, similar to the location of the benzothiazole ring of zopolrestat in the crystal structure. The binding models of zopolrestat, ponalrestat, zenarestat, WAY-122124, and the analogues with succinimide moieties suggest that they all share the following pharmacophoric elements: (1) an aromatic ring with a carboxylate or a succinimide group oriented within the oxyanion well, making hydrogen bonding interactions with Y48 hydroxyl and the N$_\epsilon$ of H110; (2) an aromatic ring attached to the acidic moiety positioned in the substrate binding region opposite W20; (3) an aromatic ring (benzothiazole or halobenzyl moiety) in a hydrophobic pocket formed between L300 and W111 (Figures 2 and 3). The inhibitors with a spirosuccinimide group, with the exception of WAY-124276, are all quite similar in their sensitivity to the mutation of W20 → A, indicating that these inhibitors derive a major portion of their binding affinity from their interactions with it. These same inhibitors also appear to be sensitive toward W111A mutant, revealing the significance of W111 interactions toward their affinity.

The crystal structure of tolrestat[2] shows that its carboxylic acid functionality binds in the same location as that of zopolrestat, while the 5-trifluoromethyl-6-methoxynaphthyl ring is positioned perpendicular to W111. In this orientation, the naphthyl ring of tolrestat is perpendicular to the plane of zopolrestat's benzothiazole ring. Consistent with this positioning, the mutation of W111 to tyrosine and alanine does not have a measurable impact on tolrestat's binding affinity (Table 1). The mutation of W20 to alanine, however, decreases its affinity by 4 orders of magnitude,[5] indicating that W20 plays a major role in defining the binding pocket for tolrestat. Our docking calculations have generated a binding model of tolrestat similar to the one observed in the crystal structure.[2]

The binding models of imirestat, WAY-121365, and WAY-120823 have an orientation similar to that described for sorbinil.[2] In these models, the spirohydantoin

Table 2. Relative Affinities of Zopolrestat in the Four Mutants

mutant	experimental IC$_{50}$ ratio (IC$_{50}^{MUT}$/IC$_{50}^{WT}$)	ΔG_{exp}[a] (kcal/mol)	carbon surface[b] area change (Å^2)	$\Delta\Delta E^{av}_{FEP}$[c] (kcal/mol)
W20Y	1.3	0.2	3	1.0 ± 1.0
W20A	838	4.0	−19	10.5 ± 2.0
W111Y	1	0.0	−0.4	4.0 ± 2.0
W111A	387	3.5	−3.7	14.0 ± 2.0

[a] ΔG_{exp} calculated from the IC$_{50}$ ratios using the following expression: $\Delta G_{exp} = -RT \ln(IC_{50}^{MUT}/IC_{50}^{WT})$. [b] As an approximation of the hydrophobic surface area buried upon binding, the decrease in carbon atom solvent accessible surface area was calculated as the mutant/inhibitor complex minus the native/inhibitor. carbon surface area change (CSA) = (mutant/inhibitor complex CSA) − (native/inhibitor complex CSA). [c] Free energy perturbation calculations were used as a way to estimate the difference in average interaction energy between zopolrestat and the wild type relative to the mutant.

or the spirosuccinimide moiety occupies the oxyanion well and the aromatic portions interact primarily with W20. These inhibitors, however, do not possess a second binding element like the benzothiazole or halobenzyl moiety found in the analogues of zopolrestat, ponalrestat, zenarestat, WAY-122124, ARI-509, and WAY-124276. The absence of a second binding element reduces the size of the inhibitor, causing them to be more sensitive to changes in the environment of the binding pocket, as indicated by the relatively large decrease in binding affinities of these inhibitors with the four mutants (Table 1). The difference in the change in affinities of these four inhibitors (**8−11**) for W20Y indicates that the interaction of the spirohydantoin moiety of imirestat and sorbinil with tryptophan is only marginally more favorable than its interaction with tyrosine.

The active-site residues of the native enzyme and the mutants with the corresponding predicted docking orientations of ARI-509 are shown in Figure 3. Our calculations place ARI-509 in an orientation similar to that of zopolrestat in the native enzyme and all the four mutants. One of the spirosuccinimide oxygens of ARI-509 interacts with the NH of W111. The nitrogen in this moiety interacts with the Nϵ of H110. The distance and angle for this interaction are 2.7 Å and 140.5°. The other oxygen of the spirosuccinimide moiety interacts with the hydroxyl of Y48 (3.0 Å, 152°).

The experimentally determined relative IC$_{50}$ values, free energy changes estimated based on these IC$_{50}$ values, calculated carbon atom surface area change (CSA), and the results from molecular dynamics/free energy perturbation calculations for zopolrestat are assembled in Table 2. The experimental free energy change is estimated using the expression $\Delta G_{exp} = -RT \ln(IC_{50}^{MUT}/C_{50}^{WT})$. As an approximation of the hydrophobic surface area buried upon binding, the decrease in carbon atom solvent accessible surface area was calculated as the mutant/inhibitor complex minus the free inhibitor. These numbers were then scaled relative to the native/inhibitor by subtracting the native/inhibitor carbon accessible surface areas. The net result is the difference in CSA between the native/inhibitor and mutant/inhibitor complex. For zopolrestat, the CSA changes correlated well with the relative IC$_{50}$ values. That is, mutants with higher IC$_{50}$ ratios accommodated the carbons of the inhibitor less effectively. Similar trends were observed for WAY-121365, although to a

Table 3. Relative Affinities of WAY-121365 and Zenarestat in the Four Mutants

mutant	experimental IC$_{50}$ ratio	carbon surface area change[a] (Å^2)
	WAY-121365	
W20Y	3	1.8
W20A	1673	−6.1
W111Y	773	1.0
W111A	2732	−2.9
	Zenarestat	
W20Y	2.5	−2.9
W20A	448	−8.3
W111Y	12	−6.6
W111A	786	−20.6

[a] As an approximation of the hydrophobic surface area buried upon binding, the decrease in carbon solvent accessible surface area was calculated as the mutant/inhibitor complex minus the free inhibitor.

smaller extent (Table 3). In the case of zenarestat, the calculated changes in surface were significantly correlated with the IC$_{50}$ ratios (Table 3). Average interaction energies calculated using free energy perturbation techniques are tabulated in Table 2. These values were calculated by taking the difference in the average interaction energy change for each mutation in solution for the isolated enzyme versus that for the enzyme−inhibitor complex. The thermodynamic cycle in Figure 4 shows the associated free energy changes for the native and a representative example of a mutant (AR$_{W20A}$) enzyme with zopolrestat. The experimentally observable process for the free energy of association for the native enzyme (AR) and mutant enzymes with zopolrestat are represented by ΔG_A and ΔG_B, respectively. We can only simulate processes that estimate the free energy change for perturbing the native to the mutant (ΔG_C and ΔG_D). From the thermodynamic cycle in Figure 4 it follows that

$$\Delta G_C + \Delta G_B = \Delta G_A + \Delta G_D \qquad (1)$$

and therefore

$$\Delta G_B - \Delta G_A = \Delta G_D - \Delta G_C \qquad (2)$$

Since our goal was to estimate average interaction energies we used free energy perturbation calculations for short durations to estimate the difference in average interaction energy between zopolrestat and the wild type relative to the mutant. Thus ΔG_C is approximated by average interaction energy ΔE^{av}_C, and ΔG_D is approximated by average interaction energy ΔE^{av}_D. The average interaction energy difference for perturbing the native to the mutant in the enzyme:NADP$^+$ binary complex and enzyme:NADP$^+$:zopolrestat quaternary complex using free energy perturbation calculations was carried out as outlined in the Methods section. Thus the interation energy changes for mutating W20 → Y20, W20 → A20, W111 → Y111, and W111 → A111 in the enzyme:NADP$^+$:inhibitor complex and also in the enzyme:NADP$^+$ complex in both forward ($\lambda = 1 \rightarrow 0$) and backward ($\lambda = 0 \rightarrow 1$) directions were calculated. The average interaction energy difference ($\Delta\Delta E^{av}_{FEP}$) shown in Table 2 was derived by calculating the difference of the average of the forward and backward free energy
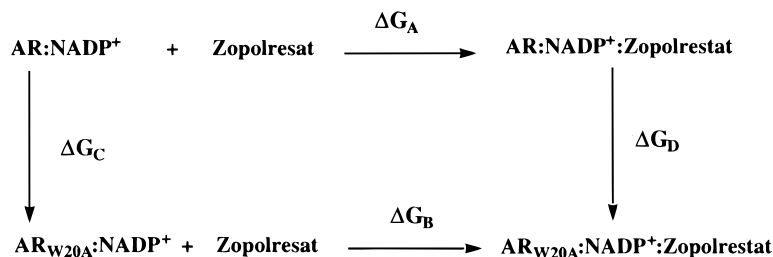
Figure 4. Thermodynamic cycle for the association processes for the native aldose reductase (AR) and the W20A mutant (AR$_{W20A}$). The thermodynamic cycle in this figure shows the associated free energy changes for the native and a representative example of a mutant enzyme with zopolrestat. The experimentally observable process for the free energy of association for the native enzyme (AR) and mutant enzymes with zopolrestat are represented by ΔG_A and ΔG_B, respectively. We can only simulate processes that estimate the free energy change for perturbing the native to the mutant (ΔG_C and ΔG_D).
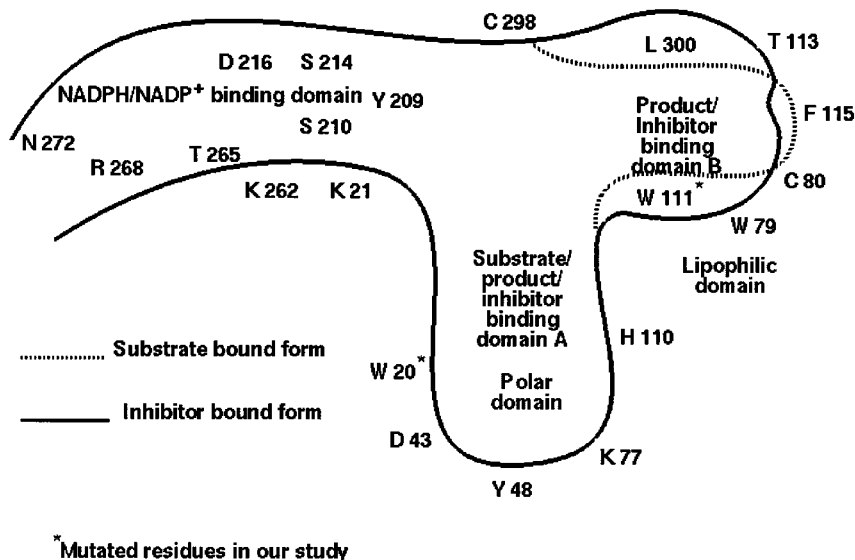

Figure 5. A cross section of the aldose reductase cofactor, substrate, and inhibitor sites is shown. The left-hand side of the schematic shows the NADPH/NADP+ binding site. Domain A is located at the bottom of the binding site and is formed by residues W20, D43, Y48, K77, and H110. This region accommodates acid functionalities including carboxylates, spirosuccinimides, and spirohydantoins. Domain B is located at the top right corner of the binding site and is formed by nonpolar residues W79, W111, C80, F115, T113, and L300. This fairly nonpolar region of the binding site accommodates the benzothiazole ring of zopolrestat and WAY-124276; the halogenated benzyl rings of ponalrestat, zenarestat, WAY-122124, and ARI-509; and the substituted naphthyl ring of tolrestat. For more details, see the text.

perturbations of the AR:NADP$^+$:zopolrestat quaternary complex and the enzyme:NADP$^+$ binary complex.

$$\Delta\Delta E^{av}_{FEP} = \Delta E^{av}_{AR:NADP+}:\text{zopolrestat}$$
$$(WT \rightarrow mutant) - \Delta E^{av}_{AR:NADP+} (WT \rightarrow mutant) \quad (3)$$

These calculated average interaction energy differences were of the same sign and relative magnitudes as the relative IC$_{50}$ values for zopolrestat.

As an approximate method for estimating lipophilic effects in these mutation studies, the accessible surface area of the carbon atoms of the small molecule inhibitors was calculated for mutant-inhibitor complex and for each inhibitor. These calculations roughly estimate the change in surface area of the buried lipophilic atoms. If a mutation increases the amount of buried lipophilic surface area, then it is assumed that the IC$_{50}$ for the mutant would decrease (i.e., increase binding). This simple model was able to explain the results for most of the inhibitors studied. The logarithm of the IC$_{50}$ ratio was correlated with the calculated change in lipophilic surface area, and in nearly all cases the correlation coefficient (r^2) was found to be greater than 0.50 (Table 4). For ponalrestat, zenarestat, and tolrestat the cor-

Table 4. Correlation Coefficients[a] for the Aldose Reductase Inhibitors

inhibitor	r^2
zopolrestat	0.66
ponalrestat	0.99
zenarestat	0.75
WAY-122124	0.70
WAY-124276	0.06
ARI-509	0.52
tolrestat	0.77
imirestat	0.36
sorbinil	0.01
WAY-121365	0.40
WAY-120823	0.52

[a] As an approximation of the hydrophobic surface area buried upon binding, the decrease in carbon solvent accessible surface area was calculated as the mutant/inhibitor complex minus the free inhibitor. The logarithm of the IC$_{50}$ ratio was correlated with the calculated change in carbon atom surface area for these compounds with each mutant. The correlations suggest that the change in the hydrophobic character of the active site is related to the ability of the mutants to bind the inhibitors.

relation coefficients are greater than 0.75. These observations imply that binding orientations found for these compounds with each mutant were reasonable and that the stabilization or destabilization was due to lipophilic

effects. Other cases that had poor correlations, such as sorbinil and WAY-124276, have mechanisms of stabilization that are due to other effects such as hydrogen bonding.

The correlation coefficients for the log of the IC_{50} ratios and the CSA were greater than 0.35 for all compounds except WAY-124276 and sorbinil. Imirestat and WAY-121365 were the only compounds with r^2 values between 0.35 and 0.5. The correlations suggest that the change in the hydrophobic character of the active site was related to the ability of the mutants to bind the inhibitors.

Discussion

The structural analysis of the substrate-bound[3] and the inhibitor-bound forms[1-3] of aldose reductase suggests that conformations of the enzyme in these forms are quite different and appear to have one binding domain for the substrate and one or two domains for an inhibitor. These domains are shown schematically in Figure 5. The NADPH/NADP+ domain is quite constant in the substrate- and the inhibitor-bound forms. We have labeled the substrate binding domain as domain A or the polar domain. In this domain, W20, D43, Y48, K77, and H110 are present, making this domain very polar and facilitating the accommodation of acidic functionalities such as carboxylic acids, spirosuccinimides, and spirohydantoins. In the inhibitor-bound form of the enzyme, the nonpolar moieties of the molecule such as benzothiazole, halogenated benzyl group, and substituted naphthyl rings occupy the second domain, which we labeled as domain B or the lipophilic domain. This domain is lined by W111, W79, C80, F115, T113, and L300, which make this domain fairly nonpolar.

Our analysis of the binding pockets of aldose reductase was qualitatively similar to that of Urzhumtsev et al.[2] These investigators classified the binding site into two regions. The first of these is a polar region with residues W20, Y48, and H110 and the nicotinamide moiety of NADP+, which accommodates the anionic carboxylate of tolrestat and the spirohydantoin of sorbinil. The second region is a nonpolar site with residues W111, T113, Y115, and L300, which accommodates the nonpolar 5-trifluoromethyl-6-methoxynaphthyl ring of tolrestat. Urzhumtsev et al.[2] proposed that the specificity for the inhibitor binding was due to inhibitor-enzyme interactions at this nonpolar site.

The quantitative assessment of the average interaction energies using free energy perturbation calculations for zopolrestat bound in the native form and with the four mutants generated from the native enzyme show that the average interaction energy differences have the same trend as the experimental relative binding affinities computed from the IC_{50} values and hence lend support to our model. The changes in carbon atom surface area, also consistent with the model, correlate well with the relative IC_{50} values.

Conclusion

We have been able to successfully generate an atomic resolution model for the zopolrestat-bound form of aldose reductase, which appears to be very similar to the published crystal structure.[1] We have used this model to generate W20A, W20Y, W111A, and W111Y mutant structures. The models of the mutant proteins allowed us to generate binding models of four representative classes of inhibitors, which, with the aid of carbon atom surface area change calculations, correlate with their binding affinities.

We have proposed a pharmacophoric hypothesis for the binding of four structurally distinct classes of inhibitors. This proposed hypothesis is supported by the estimation of relative binding affinities with the aid of carbon surface area calculations for the representative compounds from these four distinct classes of inhibitors.

References

(1) Wilson, D. K.; Tarle, I.; Petrash, J. M.; Quicho, F. A. Refined 1.8 Angstroms structure of human aldose reductase complexed with the potent inhibitor zopolrestat *Proc. Natl. Acad. Sci. U.S.A.* **1993**, *90*, 9847−9851.

(2) Urzhumtsev, A.; Tete-Favier, F.; Mitschler, A.; Barbanton, J.; Parth, P.; Urzhumtseva, L.; Biellmann, J−F.;. Podjarny, A. D.; Moras, D. A 'specificity' pocket inferred from the crystal structures of the complexes of aldose reductase with pharmaceutically important inhibitors tolrestat and sorbinil. *Structure* **1997**, *5*, 601−612.

(3) Harrison, D. H.; Bohren, K. M.; Ringe, D.; Petsko, G. A.; Gabbay, K. H. An anion binding site in human aldose reductase: Mechanistic implications for the binding of citrate, cacodylate, and glucose-6-phosphate. *Biochemistry* **1994**, *33*, 2011−2020.

(4) DesJarlais, R. L.; Sheridan, R. P.; Seibel, G. L.; Dixon, J. S.; Kuntz, I. D.; Venkataraghavan, R. Using shape complementarity as an initial screen in designing Ligands for a receptor binding site of known three-dimensional structure. *J. Med. Chem.* **1988**, *31*, 722-&29.

(5) Hohman, T. C.; ElKabbani, O.; Malamas, M. S.; Lai, K.; Putilina, T.; McGowan, M. H.; Carper, D. A. Probing the inhibitor binding site of aldose reductase with site- directed mutagenesis. *Eur. J. Biochem.* **1998**, *256*, 310−316.

(6) Weiner, S. J.; Kollman, P. A.; Case, D. A.; Singh, U. C.; Ghio, C.; Alagona, G.; Profeta,.; S.; Weiner, P. A New Force Field for Molecular Mechanical Simulation of Nucleic Acids and Proteins. *J. Am. Chem. Soc.* **1984**, *106*, 765−784.

(7) Pearlman, D. A.; Case, D. A.; Caldwell, J. C.; Seibel, G. L.; Singh, U. C.; Weiner, P.; Kollman, P. A. AMBER(4.0); University of California, San Francisco, 1991.

(8) Kuhl F. S.; Crippen, G. M.; Friesen D. K. A combinatorial algorithm for calculating ligand binding. *J. Comput. Chem.* **1984**, *5*, 24−34.

(9) Smellie A. S.; Crippen, G. M.; Richards, W. G. Fast drug-receptor mapping by site-directed distances − A novel method of predicting new pharmacological leads. *J. Chem. Inf. Comput. Sci.* **1991**, *31*, 386−392.

(10) Gasteiger, J.; Marseilli, M. Iterative partial equalization of orbital electronegativity − a rapid access to atomic charges. *Tetrahedron* **1980**, *36*, 3219−3228.

(11) Kitchen, D. B.; Hirata, F.; Kofke, D. A.; Westbrook, J. D.; Levy, R. M. Conserving Energy During Simulations of Water, Proteins and Proteins in Water. *J. Comput. Chem.* **1990**, *11*, 1169.

(12) Connoly, M. L. Solvent-accessible surfaces of proteins and nucleic acids. *Science* **1983**, *221*, 709−713.

(13) Jorgensen, W. L.; Chandrasekhar, J.; Madura, J. D.; Impey, R. W.; Klein, M. L. Comparison of simple potential functions for simulating liquid water. *J. Chem. Phys.* **1983**, *79*, 926−935.

(14) Singh, S. B.; Ajay; Wemmer, D. E.; Kollman, P. A. Relative binding affinities of distamycin and its analogue to DNA: Comparison of simulation results with experiment. *Proc. Natl. Acad. Sci., U.S.A.* **1994**, *91*, 7673−7677.

(15) Singh, U. C.; Brown, F.; Bash, P.; Kollman, P. A. An approach to the application of free energy perturbation methods using molecular dynamics: applications to the transformations of $CH_3OH \rightarrow CH_3CH_3$, $H_3O^+ \rightarrow NH_4^+$, glycine $\rightarrow$ alanine, and alanine $\rightarrow$ phenylalanine in aqueous solution and to $H_3O + (H_2O)_3 \rightarrow NH_4+(H_2O)_3$ in the gas phase. *J. Am. Chem. Soc.* **1987**, *109*, 1607−1614.

(16) Malamas, M. S.; Hohman, T. C.; Millen, M. Novel Spirosuccinimide aldose reductase inhibitors derived from isoquinoline-1,3-diones: 2-[(4-bromo-2- fluorophenyl)-methyl]-6-fluorospiro-[isoquinoline-4(1H),3′pyrrolidine]- 1,2′,3,5′(2H)-tetrone and congeners. 1. *J. Med. Chem.* **1994**, *37*, 2043−2058.